Optimization of interpass annealing for a minimum recrystallized grain size and further grain refinement towards nanostructured AA6063 during equal channel angular pressing

Shadabroo, MS; Eivani, AR; Jafarian, HR; Razavi, SF; Zhou, J

DOI
10.1016/j.matchar.2015.12.018

Publication date
2016

Document Version
Final published version

Published in
Materials Characterization

Citation (APA)
Shadabroo, MS., Eivani, AR., Jafarian, HR., Razavi, SF., & Zhou, J. (2016). Optimization of interpass annealing for a minimum recrystallized grain size and further grain refinement towards nanostructured AA6063 during equal channel angular pressing. *Materials Characterization*, *112*, 160-168. https://doi.org/10.1016/j.matchar.2015.12.018

Materials Characterization 112 (2016) 160–168

Contents lists available at ScienceDirect

Materials Characterization

journal homepage: www.elsevier.com/locate/matchar

Optimization of interpass annealing for a minimum recrystallized grain size and further grain refinement towards nanostructured AA6063 during equal channel angular pressing

M.S. Shadabroo [a], A.R. Eivani [a,*], H.R. Jafarian [a], S.F. Razavi [b], J. Zhou [c]

[a] School of Metallurgy and Materials Engineering, Iran University of Science and Technology (IUST), Tehran, Iran
[b] Material Engineering Group, Islamic Azad University, Science and Research Branch, Kermanshah, Iran
[c] Department of Biomechanical Engineering, Delft University of Technology, Mekelweg 2, 2628 CD Delft, The Netherlands

ARTICLE INFO

Article history:
Received 6 October 2015
Received in revised form 13 December 2015
Accepted 16 December 2015
Available online 18 December 2015

Keywords:
Grain structure
Grain boundary angle
Nanostructure
Equal channel angular pressing
AA6063

ABSTRACT

Grain structure evolving during severe plastic deformation (SPD) and interpass annealing strongly influences grain refinement occurring during subsequent SPD. The aim of this research was to determine an optimum interpass annealing condition that could lead to the formation of a nanostructure of the AA6063 alloy during subsequent equal channel angular pressing (ECAP). Different interpass annealing temperatures and times as well as different prior ECAP passes were used to define an optimum annealing condition that led to a minimum grain size for further ECAP by route A. TEM confirmed the attainment of nano-scale grains with sizes around 500 nm after six passes of ECAP. EBSD revealed the majority of grain boundaries being high-angle ones.

1. Introduction

Grain structure is commonly recognized as the most important microstructural feature of a metal or an alloy. For a given chemical composition, the grain structure of a metallic material significantly affects its mechanical properties [1–9], e.g., strength, ductility, formability, fatigue resistance and creep behavior, and it affects its corrosion resistance to a certain extent. A great deal of research has been performed to establish the correlations between the grain structure of metallic materials and their physical, mechanical and corrosion properties. In addition, the grain size at the beginning of material processing and its evolution along with further processing have strong effects on the thermodynamics and kinetics of diffusion and phase transformation occurring during materials processing [10]. For example, it has been found that diffusion rate increases with decreasing grain size [10]. The initial grain size also affects the precipitation in aluminum alloys and many other alloys in terms of the sizes and distribution of precipitates as well as the kinetics of their formation [10,11]. Furthermore, the initial grain size is one of the critical material microstructure parameters that influences the thermodynamics and kinetics of both static and dynamic recrystallization [4,12]. In fact, the resulting grain size after either static recrystallization or dynamic recrystallization is strongly dependent on the initial grain size in the starting microstructure [12]. Considering recrystallization in its simplest form, i.e., by nucleation and growth, it is generally accepted that fine-grained materials recrystallize more rapidly than coarse ones [12]. Moreover, the resulting grain size originating from an initially finer structure is finer than the one from a coarse initial grain structure. The initial grain size is said to affect the rate of recrystallization in several ways. The stored energy of a deformed metal increases with reducing grain size [12]; as grain boundaries are the favored nucleation sites [12], the number of available nucleation sites is larger for a fine-grained material. Similar observations have been made in the investigations on dynamic recrystallization during equal channel angular pressing (ECAP).

It is such a significant effect of the initial grain size on the properties of metallic materials and on the kinetics of phase transformation that has led many researchers to search for options to achieve grain refinement. In addition to the approaches applicable during casting and solidification, e.g., maximizing cooling rate and adding grain-refining agents, thermomechanical processing [13,14] has been widely used for grain refinement in deformable metals and alloys. Among different metal-forming techniques, severe plastic deformation (SPD) has demonstrated its unique capabilities mainly because the amount of strain that can be accumulatively imposed is in principal unlimited [15]. Equal channel angular pressing (ECAP) is the most widely used SPD technique [16,17] to create ultrafine grain (UFG) structures [16,17]. The effects of ECAP processing parameters [15,17], such as the number of passes, die angle, deformation route and back pressure on grain refinement have been extensively investigated. However, to the

* Corresponding author.
E-mail address: aeivani@iust.ac.ir (A.R. Eivani).

http://dx.doi.org/10.1016/j.matchar.2015.12.018
1044-5803/

Table 1
Chemical composition of the AA6063 alloy used in this study in comparison with the nominal composition of the alloy.

Element (wt.%)	Al	Mg	Si	Fe	Cu	Mn	Cr	Zn	Ti
AA6063 used in this study	Balance	0.84	0.57	0.31	0.03	0.04	0.03	0.10	0.03
Nominal composition of AA6063	Balanced	0.45–0.9	0.2–0.6	Max 0.35	Max 0.1	Max 0.1	Max 0.1	Max 0.1	Max 0.1

authors' best knowledge, there has been no systematic investigation on the effect of the initial grain size on the formation of nanostructures in SPD. In addition, despite of extensive existing knowledge on recrystallization and grain growth, there is very little investigation on the optimization of deformation and annealing conditions towards acquiring minimum recrystallized grain size while, it has been shown recently that the initial grain size may be significantly effective on the evolution of microstructure during subsequent deformation [18].

The aim of the present research was to contribute to filling this knowledge gap. It was hypothesized that the initial grain size would significantly affect the formation of nanostructures and their sizes during SPD. It was thus necessary to engineer the initial microstructure in order to achieve the finest possible recrystallized structure during interpass annealing for the primary purpose of stress relieving, thereby realizing a nano-sized grain structure during further ECAP passes. To confirm this hypothesis, an investigation was performed on the effect of annealing condition (temperature and time) on the fineness of recrystallized grain structure. Optimally annealed samples were subjected to further ECAP and the resultant grain structures were examined in terms of the sizes of nano-scale grains and the fraction of high angle grain boundaries.

2. Experimental procedure

The AA6063 aluminum alloy was received in the form of extruded rods with a diameter of 100 mm. The chemical composition of the rods in comparison to the nominal composition of the alloy is given in Table 1. The rods were machined into cylindrical samples with a length of 120 mm and a diameter of 20 mm. The samples were annealed at 550 °C for 30 min to remove the effects of deformation induced during the previous step of materials processing.

ECAP was performed using a die consisting of two round channels having an inside diameter of 20 mm and equal cross section and intersecting at an angle of 90° and an outer curved corner of 22.5°. With this ECAP setup, a strain of one could be imposed at each pass of deformation [19,20]. In the present research on the AA6063 aluminum alloy, prior to interpass annealing, ECAP was carried out at room temperature and at a ram speed of 10 mm/s for up to four passes using the route A, meaning that the billet was not rotated about its axis between passes. A 20 mm long section at each end of the sample was discarded in order to avoid the end effects on the microstructures and the rest was cut into pieces of an equal length of 10 mm.

The microstructures of all the samples were examined on the longitudinal section. Samples were annealed in a salt bath at 300, 350 and 420 °C for up to 3600 s. Their grain structures were studied using a polarized light microscope. The sample with the finest recrystallized microstructure after interpass annealing was chosen for further ECAP up to six passes.

Transmission electron microscopy (TEM) was used to investigate the formation of nanostructures during ECAP and their sizes. Discs with a diameter of 3 mm were punched and ground down to a thickness of less than 60 nm, followed by electro-polishing in a solution composed

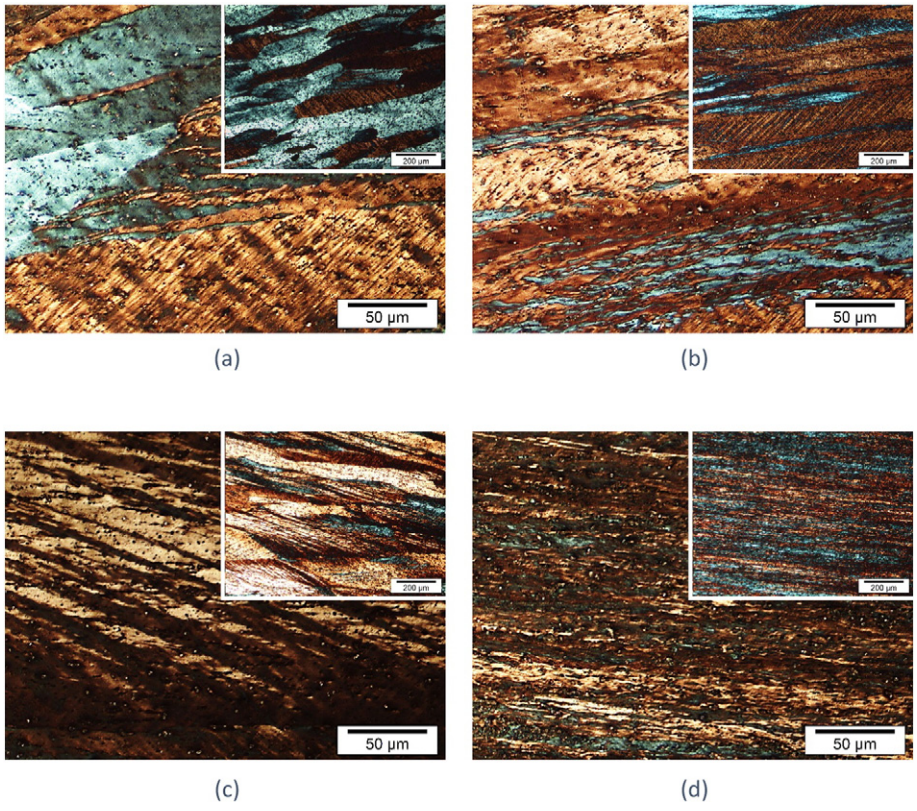

Fig. 1. Microstructures of samples after (a) one, (b) two, (c) three and (d) four ECAP passes and annealing at 300 °C for 10 s.

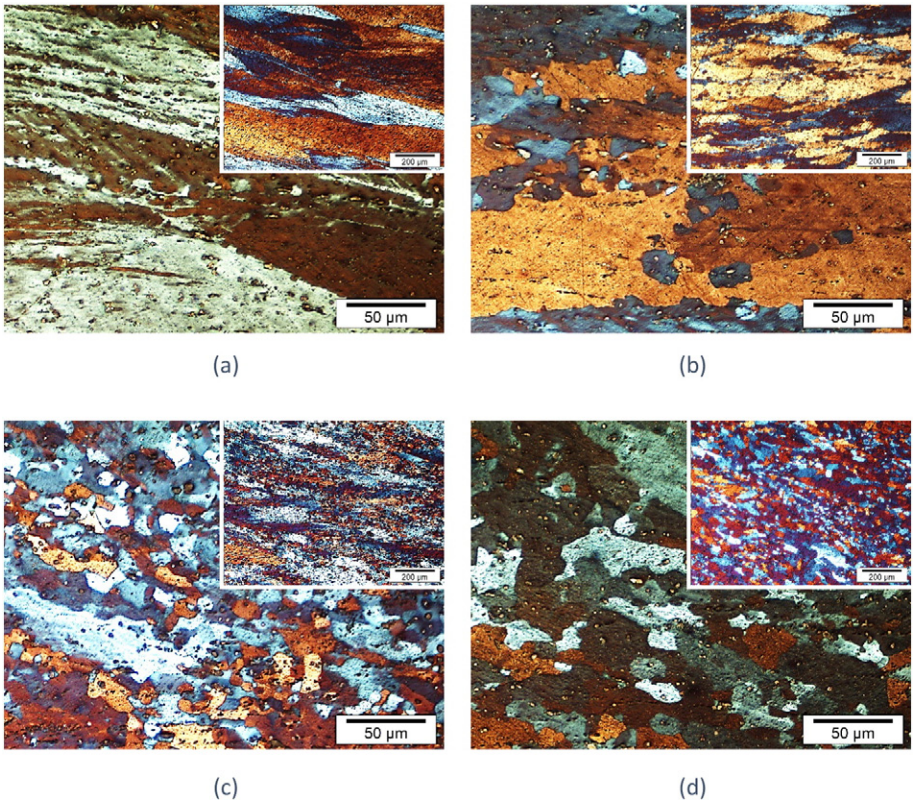

Fig. 2. Microstructures of samples after one ECAP pass and annealing at 300 °C for (a) 120, (b) 300, (c) 600 and (d) 3600 s.

of 30% nitric acid and 70% methanol and cooled to −25 °C in a double-jet polishing unit operating at 20 V. A CM30T Philips TEM operating at 300 kV was used.

For electron backscatter diffraction (EBSD) analysis, after cutting, samples were mechanically ground. Electrolytic polishing was performed at 0 °C, 17 V and a flow rate of 15 l/min for 80 s

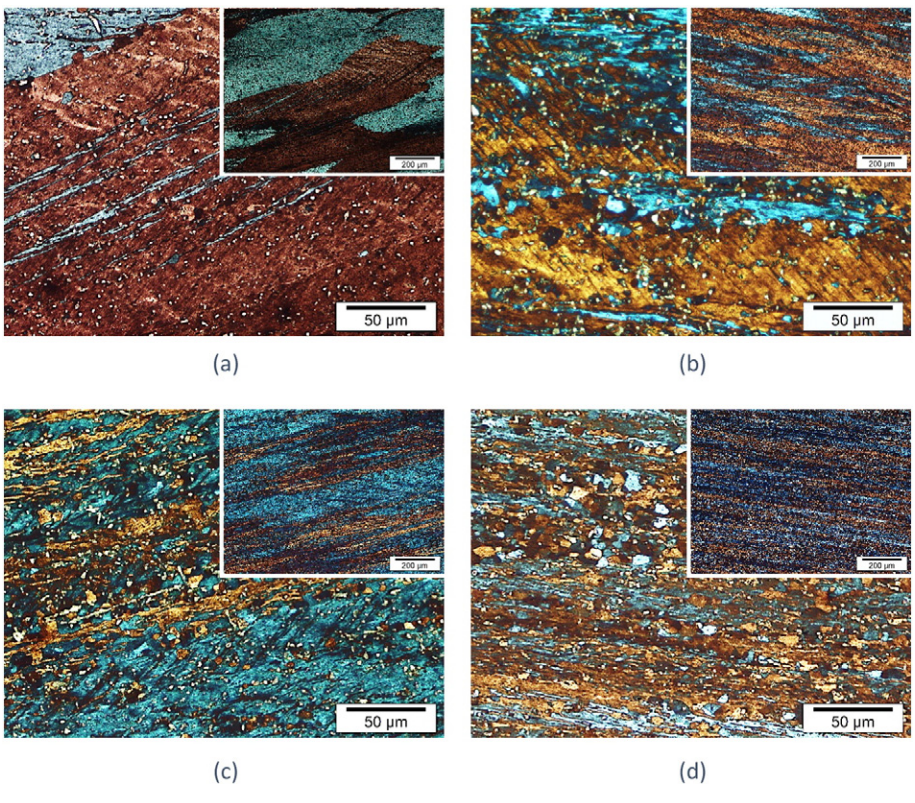

Fig. 3. Microstructures of samples after (a) one, (b) two, (c) three and (d) four ECAP passes and annealing at 350 °C for 10 s.

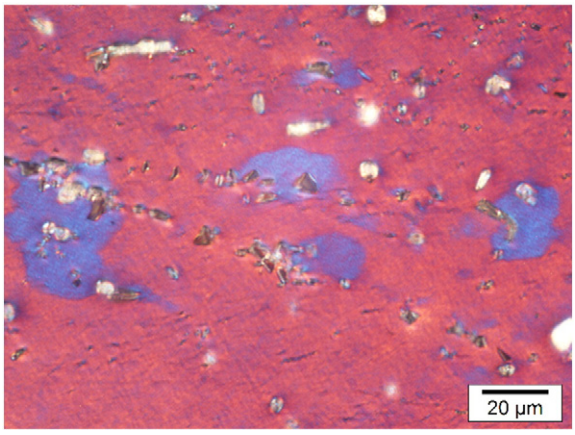

Fig. 4. Onset of recrystallization by nucleation in the sample after one ECAP pass and annealing at 350 °C for 10 s.

(electrolyte: 7.8% perchloric acid, 9% water, 73.1% ethanol and 10% butylcellulose). EBSD analysis was performed using a JEOL 6500 scanning electron microscope (SEM) at a step size of 0.1 μm. Data were analyzed using the HKL software. Misorientation angles between 2 to 15 ° were defined as low angle grain boundaries (LAGBs), while those larger than 15 ° as high angle grain boundaries (HAGBs).

3. Results and discussion

3.1. Microstructural evolution during interpass annealing after different ECAP passes

To clarify the effect of the number of ECAP passes on the fraction recrystallized, the microstructures of samples after different ECAP passes, followed by annealing at 300 °C for 10 s, as shown in Fig. 1, were first investigated. In general, none of the samples were really recrystallized, as evidenced by severely elongated grains. This indicates that annealing at 300 °C for such a short time could not provide enough activation energy or time for the occurrence of static recrystallization. Only a very small number of recrystallization nuclei could be discerned in the sample deformed through four ECAP passes, which made this sample appear to be slightly different from the other samples. This is due to a higher stored energy accumulated in this sample as a result of a significant amount of cold work, equivalent to an accumulative effective strain of 4 [19,20], and thus a higher driving force for recrystallization [21,22].

Obviously, to facilitate full recrystallization to occur at this annealing temperature, annealing time should be prolonged. The microstructures of samples after one ECAP pass and annealing at 300 °C for different times were investigated, as shown in Fig. 2. It was clear that full recrystallization would not occur unless the annealing time was extended to 3600 s. However, the application of such an annealing treatment would result in a coarse grain structure, as in this case the number density of recrystallization nuclei would be rather low according to Eq. (1). In fact, nucleation rate density $\dot{N}$ is a function of temperature T as described in Eq. (1) [12]:

$$\dot{N} = C\exp\left(-\frac{Q_N}{kT}\right) \tag{1}$$

where C is a nucleation rate constant, Q_N is the activation energy for nucleation and k is the Boltzman constant. Obviously, if annealing is performed at a low temperature, the number density of nuclei will be small and these nuclei will have to grow to form a fully recrystallized structure. The resulting microstructure must be rather coarse. Comparison of a fully recrystallized microstructure (Fig. 2d) with the microstructures obtained from annealing at higher temperatures, could clearly show that the grain structure formed during annealing at 300 °C for 3600 s was coarser, thus being undesirable for achieving a nano-scale grain structure after further ECAP. One may thus conclude

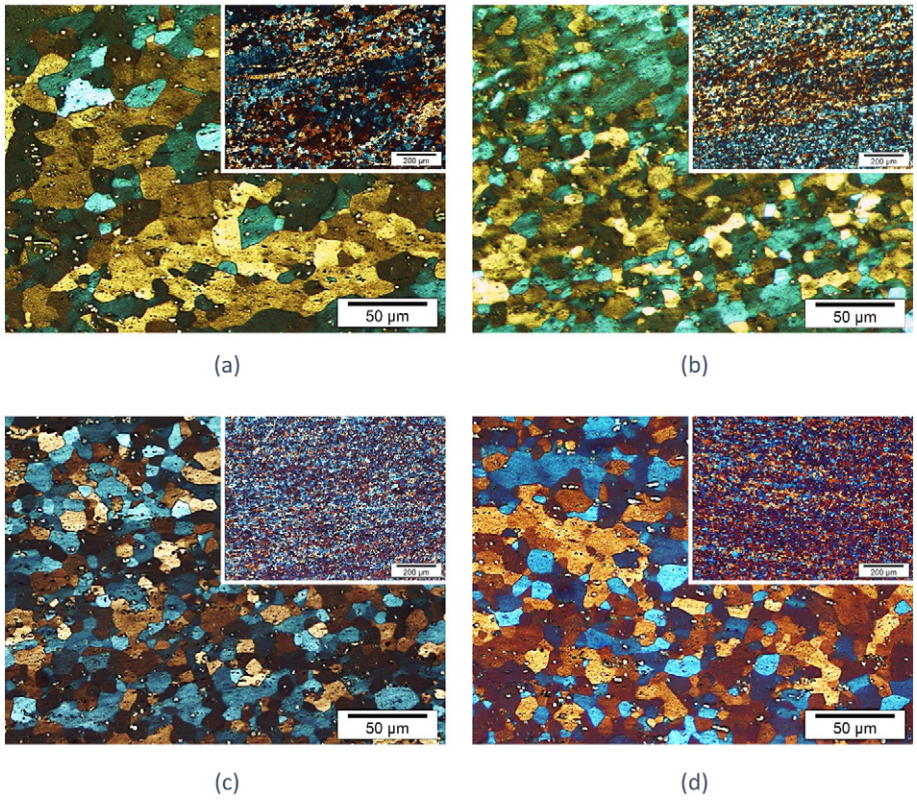

Fig. 5. Microstructures of samples after (a) one, (b) two, (c) three and (d) four ECAP passes and annealing at 420 °C for 10 s.

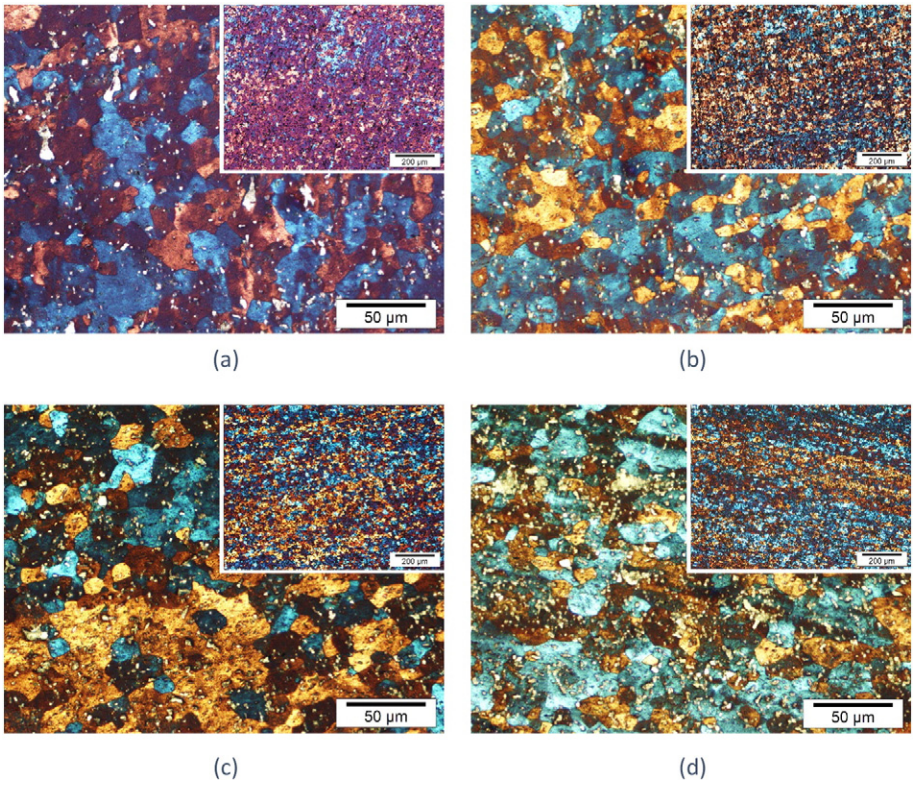

Fig. 6. Microstructures of samples after two ECAP passes and annealing at 420 °C for (a) 120, (b) 300, (c) 600 and (d) 3600 sec.

that a desirable annealing temperature is the one that allows site-saturated nucleation as the main mechanism and can realize full recrystallization within 10 s.

Based on the findings shown above, the annealing temperature was raised to 350 °C. The resulting microstructures after different ECAP passes, followed by annealing for 10 s, are presented in Fig. 3. It can be

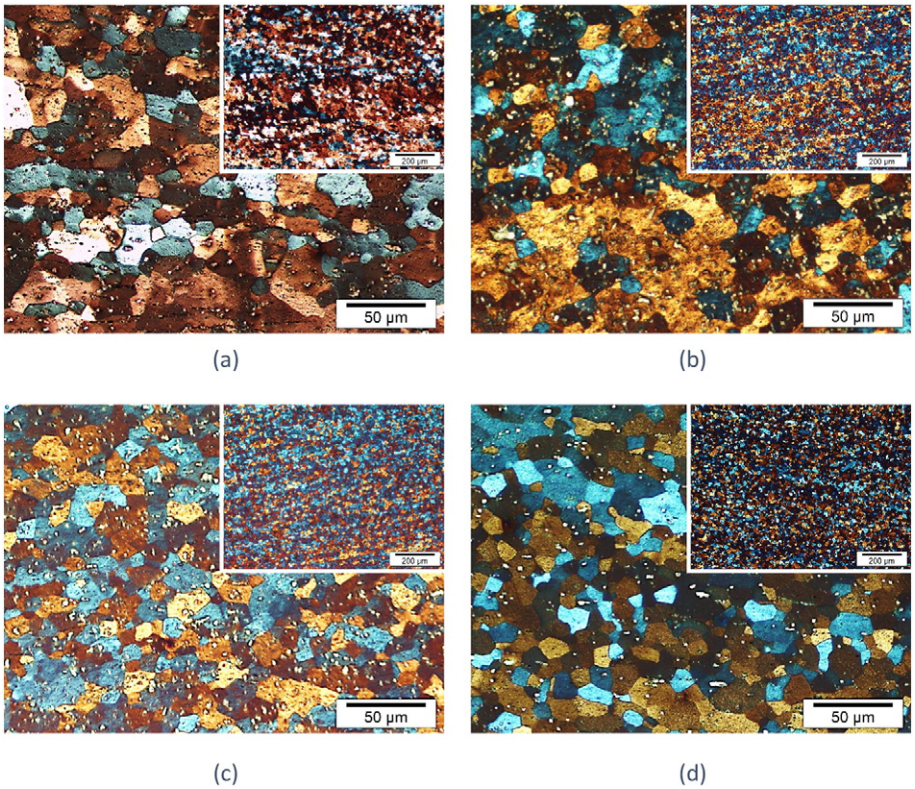

Fig. 7. Microstructures of samples after (a) one, (b) two, (c) three and (d) four ECAP passes and annealing at 420 °C for 600 s.

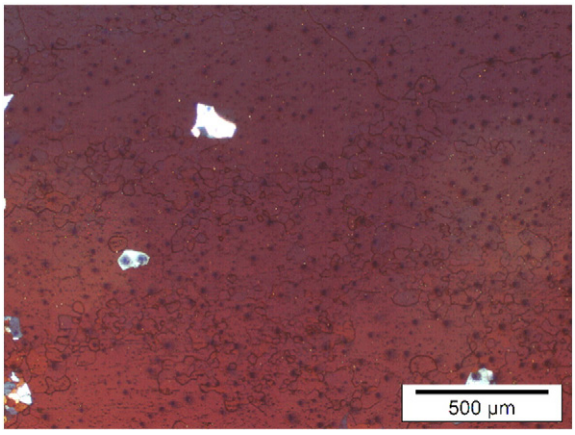

Fig. 8. Microstructures of samples after two passes ECAP and annealing at 550 °C for 6 hrs.

seen that all the samples were partially recrystallized during annealing. It was noted during the microstructure examination that for the samples after two, three and four ECAP passes, the fractions recrystallized were measurable at a magnification as presented in Fig. 3, while in the sample after one ECAP pass and annealing at 350 °C for 10 s, recrystallization was only at an early stage (Fig. 4). The fraction recrystallized gradually increased with increasing number of ECAP passes. In addition, the fractions recrystallized were obviously higher than those after ECAP under the same ECAP deformation conditions and annealing at 300 °C, as shown in Fig. 1. This is attributed to a larger number density of nuclei according to Eq. (1) and a faster growth rate at the higher temperature of annealing [12]. In addition, it was noticed that the fraction recrystallized kept increasing up to three ECAP passes, but remained almost unchanged at the fourth pass. This might be because more extensive grain refinement occurred during the fourth pass of ECAP [15], which consumed the stored energy and left a weakened driving force for subsequent static recrystallization [12]. According to the results shown above, it was decided to raise the annealing temperature further in order to explore the possibilities of obtaining finer recrystallized grain structures.

The microstructures of samples after different ECAP passes and annealing at 420 °C for 10 s are shown in Fig. 5. It can be seen that all samples were fully recrystallized. To capture a minimum recrystallized grain size, the interpass annealing treatment must be stopped right after the ECAP-deformed structure is fully recrystallized. However, apart from obtaining a fully recrystallized structure, a homogeneous distribution of temperatures, corresponding to a homogeneous distribution of microstructures, must also be achieved.

Although the samples investigated in this research were small enough to attain homogeneous temperature and microstructure distributions quickly, the samples that were to be inserted in the ECAP setup for successive ECAP deformation were on a larger scale. Therefore, in order to yield trustable results for larger-scale applications, the annealing time was extended to the limit to which significant grain growth did not occur. With increasing annealing time up to 600 s, no grain growth was recognizable (Fig. 6a – c). A further extension to 3600 s, however, indeed caused measurable grain growth (Fig. 6d). Therefore, 600 s was considered the time long enough for interpass annealing without causing significant grain growth. Thus, the temperature of 420 °C and time of 600 s were taken as an optimum interpass annealing condition to achieve a minimum recrystallized grain size.

The effect of the number of ECAP passes on the microstructure of the samples after applying the optimum annealing treatment is shown in

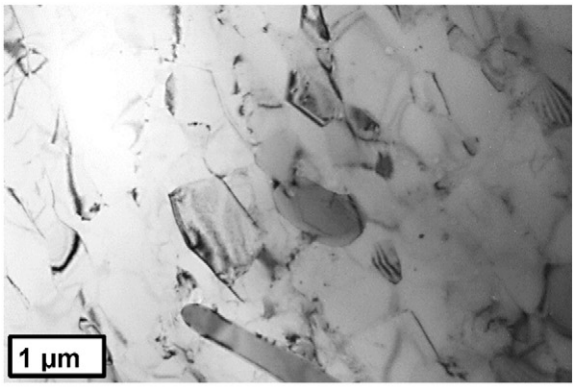

(a)

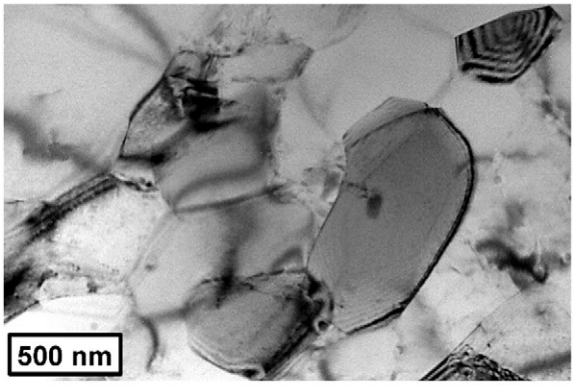

(b)

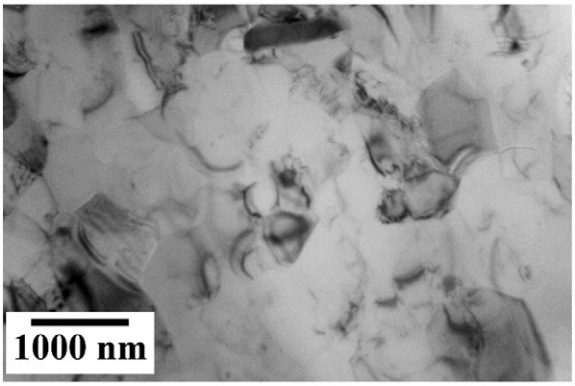

(c)

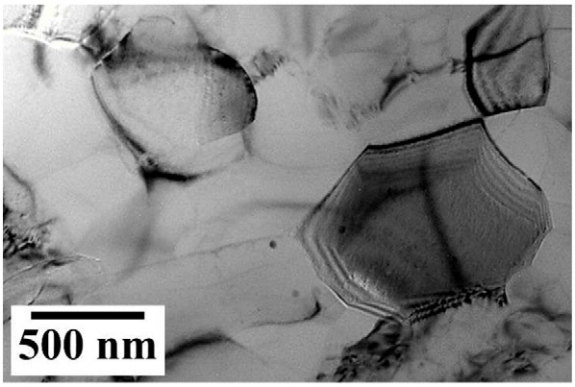

(d)

Fig. 9. (a) Low and (b) high magnefication TEM micrographs of the sample after the optimum annealing treatment, i.e., 420 °C for 10 min, followed by six ECAP passes. (c) Low and (d) high magnefication TEM micrographs of the sample after annealing at 500 °C for 6 hrs, followed by six ECAP passes.

Fig. 7. Grain size was found to decrease significantly as the number of ECAP passes increased from one to two (see Fig. 7a and b). However, further increases in the number of ECAP passes did not clearly affect the grain size and thus would not be necessary. Therefore, two ECAP passes prior to applying the optimum interpass annealing treatment was chosen as an optimum.

3.2. Development of nanostructure during subsequent ECAP

Samples with a fully recrystallized and stress-relieved grain structure after two ECAP passes and annealing at 420 °C for 600 s (Fig. 7b) were subjected to further ECAP. In addition, for the sake of comparison, another sample is annealed at 550 °C for 6 h to acquire a coarse grain structure. The resulting microstructure is shown in Fig. 8. Very extensive abnormal grain growth is obviously observed which is due to the high temperature and long time applied during annealing.

TEM micrographs of these samples after six ECAP passes are shown in Fig. 9. From Fig. 9a and b, the formation of nano-sized cell structures is clear in every region of the sample. The average cell size is around 500 nm, which is comparable with the UFG structures of aluminum alloys reported in the literature and achieved with more complex SPD processes [23,24]. The obtained microstructure from the coarse grained sample is shown in Fig. 9c and d. It is clear that a coarse nanostructure is formed with an average cell size around 700 nm.

EBSD images of the nanostructure developed during the final pass of ECAP are presented in Fig. 10. It can be seen in Fig. 10a that thorough

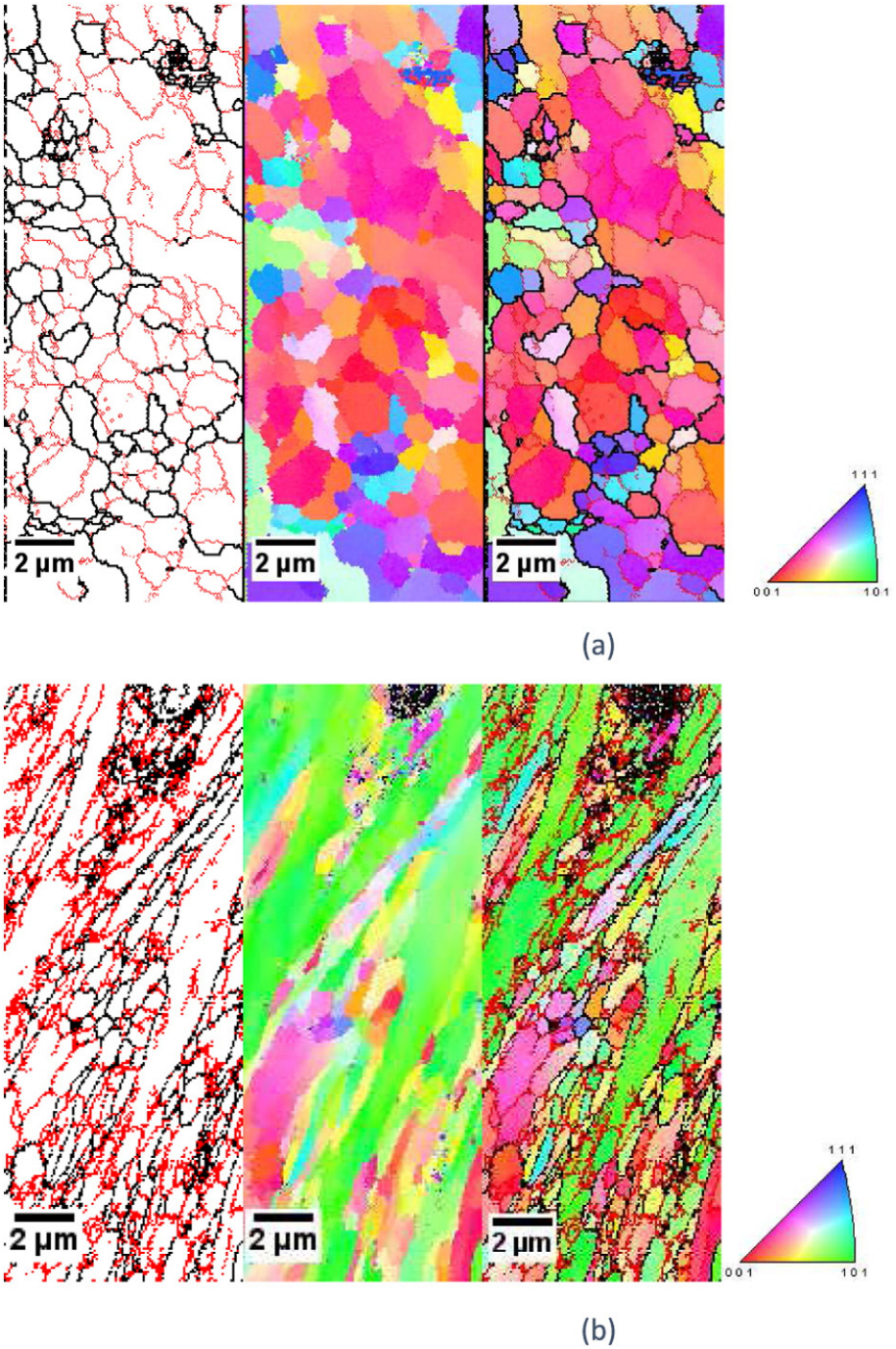

Fig. 10. EBSD images of the sample (a) after the optimum annealing treatment and six ECAP passes, (b) (a) after annealing at 550 °C for 6 hrs and six ECAP passes.

recrystallization was observed and the formation of a fine and equiaxed nanostructure with an average cell size of 530 nm was confirmed for the sample annealed at 420 °C for 10 min. The EBSD images also revealed a large fraction of high angle grain boundaries (HAGBs) between the refined grains for this sample. However, it can be seen in Fig. 10b that a coarse and elongated cell structure is developed when the sample is annealed at 550 °C for 6 h. In addition, lower fraction of HAGBs are measured for this sample in comparison to the one annealed at 420 °C for 10 min.

Misorientation angle values extracted from EBSD results are presented in Fig. 11. It is clear from Fig. 11a that the cell structure formed during ECAP is mostly composed of high angle boundaries in the case of the sample annealed at 420 °C for 10 min. In fact, more than 50% of grain boundaries had misorientation angles larger than 15 °, i.e., defined as high angle grain boundaries (HAGBs). In other words, thorough recrystallization and nanostructure formation occurred during post-annealing ECAP in the fine grain sample. It should be added that When an initial coarse grain structure is utilized, the resulting fraction of HAGBs is similar to that of fine grain structure, as indicated in Fig. 11b.

The distribution of grain sizes in the sample was extracted from EBSD results as well and they are shown in Fig. 12. It is clear from Fig. 12a that the majority of cells fell in a size range of less than 1000 nm with an average value of 530 nm. Comparison of the results with those extracted from the sample with coarser grain structure, i.e., Fig. 12b, indicates that that the average grain size is indeed significantly reduced by using the finest initial microstructure and demonstrates the efficiency of the SPD approach applied in this research.

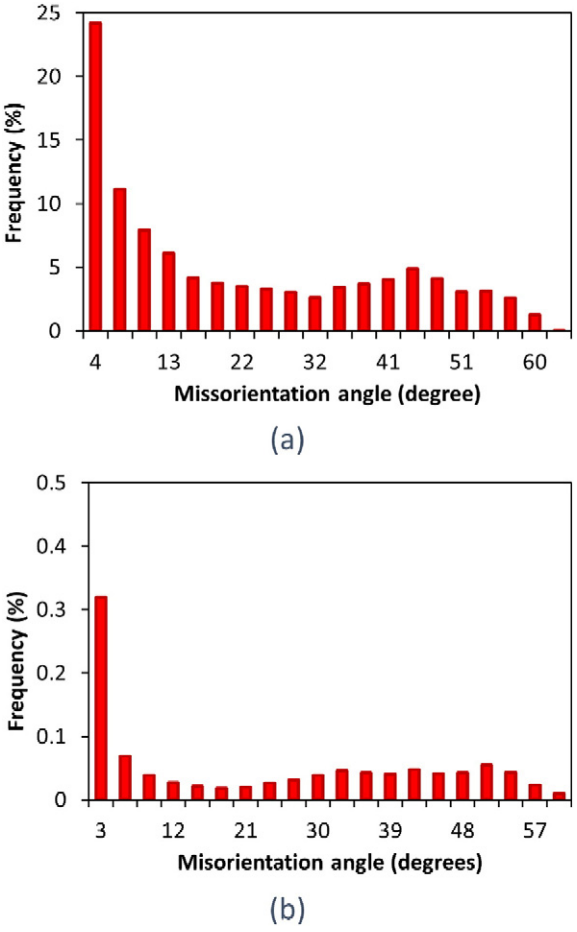

Fig. 11. Distribution of missorientation angles in the sample (a) after the optimum annealing treatment and six ECAP passes and (b) after annealing at 550 °C for 6 hrs and six ECAP passes.

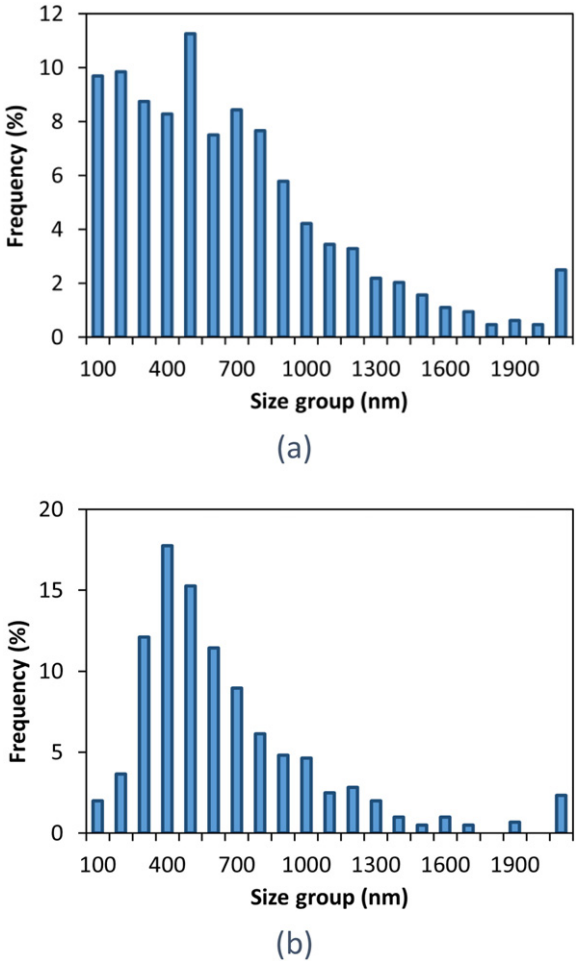

Fig. 12. Cell size distribution in the sample (a) after the optimum annealing treatment and six ECAP passes and (b) after annealing at 550 °C for 6 hrs and six ECAP passes.

4. Conclusions

To prove the hypothesis that a fine initial structure could lead to nanostructure formation during SPD, a study was conducted to achieve a fine, homogeneous grain structure of the AA6063 alloy during interpass annealing and then nanostructure after subsequent six passes of ECAP. The results obtained led to the following conclusions.

1- Interpass annealing at temperatures lower than 420 °C could not result in full recrystallization unless extensive time was allowed, which caused grain growth. The finest grain structures in the stress-relieved samples of the AA6063 alloy were obtained after annealing at 420 °C for 600 s.

2- Regarding the number of ECAP passes prior to interpass annealing, it was found that grain refinement mostly occurred during the first pass and the second pass. Further increases in the number of ECAP passes did not significantly affect the grain size after interpass annealing any more.

3- With the optimum interpass annealing, the average nanostructure size obtained after six ECAP passes was down to 530 nm, confirming the capability of ECAP by route A in achieving a nanostructure of the aluminum alloy.

Funding

No funding.

Conflict of Interest

The authors declare that they have no conflict of interest.

Acknowledgements

The authors would like to thank Prof. Nobuhiro Tsuji, Kyoto University, Japan, for providing equipment for EBSD analysis.

References

[1] R.W. Hertzberg, Deformation and fracture mechanics of engineering materials, http://cds.cern.ch/record/2589121989 (accessed September 23, 2015).
[2] L. Karthikeyan, V.S. Kumar, Relationship between process parameters and mechanical properties of friction stir processed AA6063-T6 aluminum alloy, Mater. Des. 32 (2011) 3085–3091.
[3] X. Liang, H. Li, Z. Li, T. Hong, B. Ma, S. Liu, et al., Study on the microstructure in a friction stir welded 2519-T87 Al alloy, Mater. Des. 35 (2012) 603–608.
[4] H.R. Ashtiani, M.H. Parsa, H. Bisadi, Effects of initial grain size on hot deformation behavior of commercial pure aluminum, Mater. Des. 42 (2012) 478–485.
[5] R.B. Hmida, S. Thibaud, A. Gilbin, F. Richard, Influence of the initial grain size in single point incremental forming process for thin sheets metal and microparts: Experimental investigations, Mater. Des. 45 (2013) 155–165.
[6] Y. Yang, Z. Zhang, X. Li, Q. Wang, Y. Zhang, The effects of grain size on the hot deformation and processing map for 7075 aluminum alloy, Mater. Des. 51 (2013) 592–597.
[7] S. Qu, X.H. An, H.J. Yang, C.X. Huang, G. Yang, Q.S. Zang, et al., Microstructural evolution and mechanical properties of Cu–Al alloys subjected to equal channel angular pressing, Acta Mater. 57 (2009) 1586–1601.
[8] X.H. An, S.D. Wu, Z.G. Wang, Z.F. Zhang, Enhanced cyclic deformation responses of ultrafine-grained Cu and nanocrystalline Cu–Al alloys, Acta Mater. 74 (2014) 200–214.
[9] X. An, Q. Lin, S. Wu, Z. Zhang, Improved Fatigue Strengths of Nanocrystalline Cu and Cu–Al Alloys, Mater. Res. Lett. (2015) 1–7.
[10] P. DA, K.E. Easterling, Phase Transformations in Metals and Alloys, Chapman Hall, 1992.
[11] A. Mucsi, Effect of hot rolled grain size on the precipitation kinetics of nitrides in low carbon Al-killed steel, J. Mater. Process. Technol. 214 (2014) 1536–1545.
[12] A. Rollett, F.J. Humphreys, G.S. Rohrer, M. Hatherly, Recrystallization and related annealing phenomena, Elsevier, 2004 (https://books.google.com/books?hl=en&lr=&id=52Gloa7HxGsC&oi=fnd&pg=PP1&dq=FJ+Humphreys,+M+Hatherly+(1995)+Recrystallization+and+related+annealing+phenomena.+Elsevier,+&ots=LgBadmLsgz&sig=exupTTDJW4UOV8zgaMNW9COGFkE (accessed September 23, 2015)).
[13] N.R. Kumar, J.J. Blandin, C. Desrayaud, F. Montheillet, M. Suéry, Grain refinement in AZ91 magnesium alloy during thermomechanical processing, Mater Sci Eng A 359 (2003) 150–157.
[14] J.A. Wert, N.E. Paton, C.H. Hamilton, M.W. Mahoney, Grain refinement in 7075 aluminum by thermomechanical processing, Metall. Trans. A 12 (1981) 1267–1276.
[15] R.Z. Valiev, R.K. Islamgaliev, I.V. Alexandrov, Bulk nanostructured materials from severe plastic deformation, Prog. Mater. Sci. 45 (2000) 103–189.
[16] V.M. Segal, Materials processing by simple shear, Mater Sci Eng A 197 (1995) 157–164.
[17] R.Z. Valiev, T.G. Langdon, Principles of equal-channel angular pressing as a processing tool for grain refinement, Prog. Mater. Sci. 51 (2006) 881–981.
[18] S. Valipour, A.R. Eivani, H.R. Jafarian, S.H. Seyedein, M.R. Aboutalebi, Effect of pre-deformation thermomechanical processing on the development of ultrafine grain structure during equal channel angular extrusion, Mater. Des. 89 (2016) 377–384.
[19] A.R. Eivani, A.K. Taheri, A new method for estimating strain in equal channel angular extrusion, J Mater Process Technol 183 (2007) 148–153.
[20] A.R. Eivani, A.K. Taheri, The effect of dead metal zone formation on strain and extrusion force during equal channel angular extrusion, Comput. Mater. Sci. 42 (2008) 14–20.
[21] C.Y. Yu, P.L. Sun, P.W. Kao, C.P. Chang, Evolution of microstructure during annealing of a severely deformed aluminum, Mater Sci Eng A 366 (2004) 310–317.
[22] N. Rangaraju, T. Raghuram, B.V. Krishna, K.P. Rao, P. Venugopal, Effect of cryo-rolling and annealing on microstructure and properties of commercially pure aluminium, Mater Sci Eng A 398 (2005) 246–251.
[23] I. Sabirov, M.Y. Murashkin, R.Z. Valiev, Nanostructured aluminium alloys produced by severe plastic deformation: New horizons in development, Mater Sci Eng A 560 (2013) 1–24, http://dx.doi.org/10.1016/j.msea.2012.09.020.
[24] G. Sha, K. Tugcu, X.Z. Liao, P.W. Trimby, M.Y. Murashkin, R.Z. Valiev, et al., Strength, grain refinement and solute nanostructures of an Al–Mg–Si alloy (AA6060) processed by high-pressure torsion, Acta Mater 63 (2014) 169–179, http://dx.doi.org/10.1016/j.actamat.2013.10.022.